

THE CORROSION RESISTANCE OF HEATPROOF NICKEL ALLOY IN MOLTEN FLUORIDE SALTS

*V.M. Azhazha, A.S. Bakai, Yu.P. Bobrov, V.D. Virich, T.G. Yemlyaninova, V.L. Kapustin,
K.V. Kovtun, S.D. Lavrinenko, D.G. Malykhin, I.A. Petel'guzov, M.M. Pylypenko,
V.I. Savchenko, N.A. Semyonov, A.D. Solopikhin, B.M. Shirokov*
*National Science Center "Kharkov Institute of Physics and Technology",
1 Akademicheskaya St., 61108 Kharkov, Ukraine*
E-mail: azhazha@kipt.kharkov.ua

Studies have been made into corrosion and mechanical properties of high-nickel alloys prepared at NSC KIPT on the basis of high-purity metal components. Corrosion tests of the Hastelloy-type alloy in fluoride melts at 650°C revealed formation of no films in the process of corrosion during 700 hours. The corrosion of the alloy under study in molten fluorides is characterized by a weak interaction of melt components with the alloy, by penetration of Zr and Na atoms into the alloy at a depth of 3 to 5 μm over 700 hours, by the absence of oxide films on the surface. The chromium content in the near-surface layer of the alloy decreases to a depth of 10 μm. Corrosion tests cause no essential changes in the mechanical properties of the alloy.

1. INTRODUCTION

The high-temperature homogeneous molten salt cold graphite reactor (MSGR) that was under development in the USA and the USSR [1-3] is one of the safe types of nuclear reactors. Aside from power generation, the reactor of this type is capable of realizing afterburning and transmutation of spent nuclear fuel.

In the MSGR, the part of a coolant is played by molten fluoride salts of lithium, sodium, zirconium with addition of a fissile material, e.g., uranium or plutonium fluoride. Heat-resistant and corrosion-resistant high-nickel alloys are used as structural materials for the reactor of this type. Among these alloys are the Hastelloy N-type alloy and its Russian analog KhN80MT.

Using high-purity components as the base, Hastelloy N-type alloys were smelted at the NSC KIPT; samples from these alloys were prepared for performing corrosion tests.

The aim of the present work has been to conduct corrosion tests of the samples in molten fluoride salts of zirconium and sodium.

2. MATERIALS AND INVESTIGATION TECHNIQUES

The studies were performed on the samples of a high-nickel alloy produced at NSC KIPT with the use of high-purity metal components as the base. The alloy had the following composition: Ni – base, Mo – 11.7, Cr – 6.7, Ti – 0.47, Al – 0.83, Fe – 1.5, Mn – 0.5, Si – 0.15 wt.%. The high-purity initial components with a low content of interstitial impurities, which were used for preparing the alloy, were subjected to prerefining by physical methods. The metal purification was performed by different methods. For refining of nickel, molybdenum, niobium, titanium and iron, we have used the method of vacuum electron-beam melting (EBM) at the facility described in [4]. High-vacuum annealing was

used for refining of chromium and aluminum. Manganese was refined by the vacuum distillation technique.

For alloy smelting, we have used the method of induction melting of prepared stock in the argon atmosphere of the "Kristall-603" facility. At the end of the process, a low-velocity casting into a water-cooled copper mold was performed. The resulting ingots were cut with an electrospark discharge machine to have a prismatic shape; then they were heated up to 900°C and were rolled to a thickness of 1 and 0.3 mm with intermediate annealings. The rolled strips underwent the following heat treatment: 1 – homogenizing annealing at 1100°C, a 1-hour exposure interval in air followed by water quenching (after quenching the plate surface was subjected to etching); 2 – after annealing the plates were subjected to aging at 675°C during 5 hours in the argon atmosphere [5, 6]. The samples for corrosion tests presented the 27x23x1 mm plates cut out of the rolled strip by means of the electrospark discharge machine. Before the tests the sample surface was ground using the sandpaper with a grain size of 20 μm, the edges were blunted.

Corrosion tests in air. Comparative corrosion tests of both the given alloy and the reactor stainless steel EhI-847 were conducted in air environment at temperatures of 650 and 750 C in the muffle furnace. The samples were placed in alundum boats and were periodically taken out for weighing on the microbalance VLR-20.

Tests in molten salts. The molten-salt (50ZrF₄+50NaF(mol.%)) test technique consisted in determining the degree of interaction between hastelloy samples and molten salts with a long-term isothermal holding in pyrocarbon ampoules. The tests were performed in the inert gas + high-purity argon environment. The rate of interaction between the material and the molten salts was estimated from mass variations determined by the analytical microbalance to an accuracy of 0.05 mg [7]. Metallographic methods and secondary-ion mass-spectrometry technique were used to investi-

gate the sample surfaces. Mechanical properties of the samples were also investigated. The device for tests in the salt composition includes the pressurized chamber equipped with a system pumping to a vacuum of $1 \cdot 10^{-2}$

mm Hg, the device for filling the chamber volume with argon from a vessel and the manometers for pressure measurements (see Fig. 1).

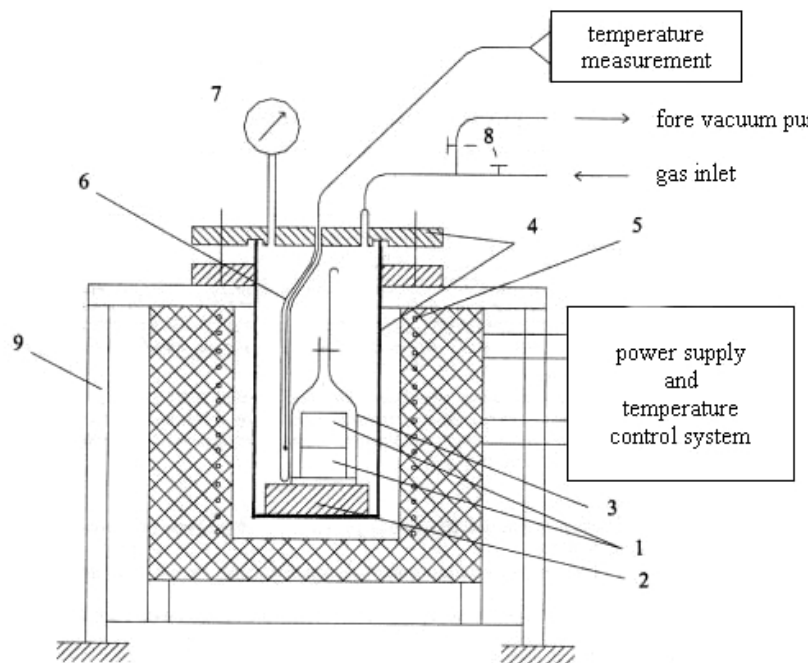


Fig. 1. Schematic of the setup for corrosion tests of Hastelloy-type alloy samples in molten fluoride salts in graphite ampoules: 1 – pyrocarbon ampoules with molten salts; 2 – sample mount, 3 – safety valve; 4 – vacuum chamber body; 5 – heating furnace, 6 – thermocouple, 7 – manometer, 8 – vacuum pumping and gas inlet system, 9 – frame

The container with pyrocarbon ampoules and samples was placed into the furnace TG-1 with a heater. The furnace was equipped with the instrumentation to maintain the assigned temperature, to measure and register its values. Before the experiment, the sample surface was degreased in gasohol, and after drying, the samples were weighed on the analytical balance. Then the samples were put into pyrocarbon ampoules, which were filled in a special chamber with a molten salt mixture at a temperature of $\sim 550^\circ\text{C}$ in the argon medium. The cross section of the ampoule filled with a solidified melt of fluorides is given in Fig. 2.

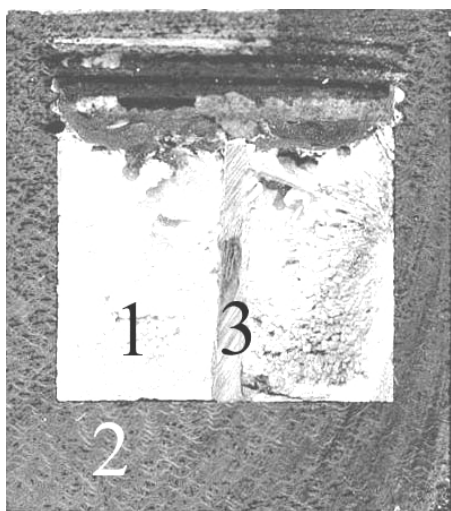


Fig. 2. The ampoule filled with solidified molten fluorides is section: 1 – solidified molten salts; 2 – pyrocarbon ampoule; 3 – alloy sample

The filled ampoules were closed by threaded covers. As the ampoules were put into the working chamber, the latter was twice pumped out to vacuum and was “washed” by argon. Then, in the argon atmosphere (1.2 MPa), the samples were heated and held at a temperature of 650°C in the molten salts during 100, 200, 500 and 700 hours. On opening the ampoules, the alloy samples were taken out, the salt remains were removed from their surface, the samples were weighed, their microstructure and mechanical properties were investigated; the X-ray diffraction analysis was also performed and variations in the chemical composition in the sample depth were studied.

The microstructure of samples was examined with the metallography microscope MMR-4. The chemical composition variations in the depth of the sample were investigated by the secondary-ion mass-spectrometry method using the MS-7201 device.

The X-ray diffraction studies of alloys were made at the DRON4-07 facility with the scintillation counter in the radiation of $\text{CuK}\alpha$ and $\text{CoK}\alpha$. The reflections were obtained using the Bragg-Brentano optical scheme. The morphology of sample surface after corrosion was examined in the electron-scan microscope REMMA-200.

The chemical composition of the salt that underwent corrosion tests was analyzed by the mass-spectrometer EhMAL-2. The tensile testing machine of type 1246R-2/2600 was used to investigate the mechanical properties of alloys in the temperature range from 20 to 650°C .

3. RESULTS AND DISCUSSION

The kinetic curves showing the increase in weight of high-nickel alloy and stainless steel samples versus time at oxidation in air during 660 h are shown in Fig. 3. It can be seen that the process of corrosion of the Hastelloy-type alloy at 650°C has a damped character, and this gives evidence for the protective mechanisms of the oxidation process. The rate of alloy oxidation is rather low. If it is assumed that the protective oxide film consists of NiO and Cr₂O₃ in the 50:50% ratio, then its thickness estimated from the sample increase in weight during 660 h will make only 1.74 μm. No delamination or flaking off of oxide films was observed. The rise in the oxidation temperature up to 750°C for the Hastelloy-type alloy also gives moderate oxidation rates; the curves of the oxidation process show the damped character. The thickness of oxide films formed during 700 h at 750°C is calculated to be approximately 6 μm.

The oxidation rate of stainless steel EI-847 is appreciably higher than that of the Hastelloy-type alloy at the two test temperatures. The calculations of the thickness of oxide films on steel at 650°C show it to be 7.7 μm af-

ter 660 hours of tests, while at 750°C the 7 to 8 μm film thickness is attained as early as in 100 h. So, our Hastelloy-type alloy [5] is a highly corrosion-resistant material that may be used in different fields of engineering.

The variation in the sample mass with time of hold in the molten salts is shown in Fig. 4. It is seen that this variation has an irregular character: at first, we observe an enhanced increase in weight for up to 250 hours of tests, and then it gradually falls off at subsequent tests during 700 hours. Evidently, this behavior reflects the complicated kinetics of interaction between fluoride salts and the Hastelloy-type alloy. Figure 5 shows the appearance of the samples (upper row, 1.3 x magnification) and morphological peculiarities of the sample surface after corrosion tests in the salt mixture during 100...700 hours (500 x magnification). The optical microscopy examination of the surface has revealed the islands of loose formations that may be the result of interaction between the molten salts and the alloy. These formations could not be removed by vacuum annealing at 650°C. Their presence is probably one of the reasons that accounts for the increase in weight.

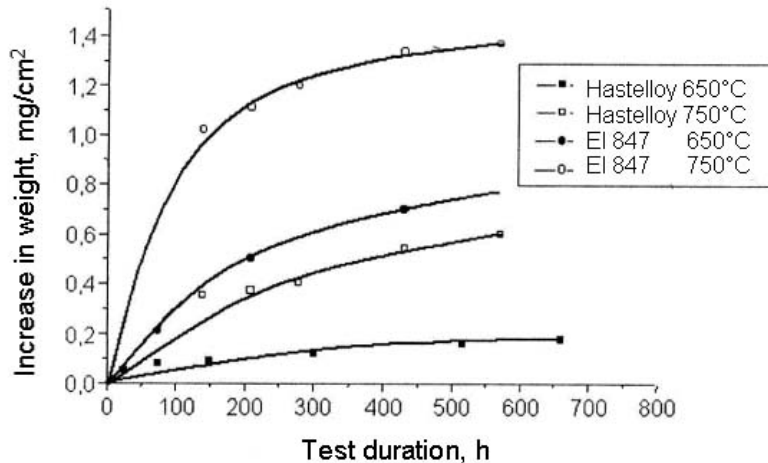


Fig. 3. Comparison between increases in weight for Hastelloy-type alloy and stainless steel EI 847 at oxidation in air

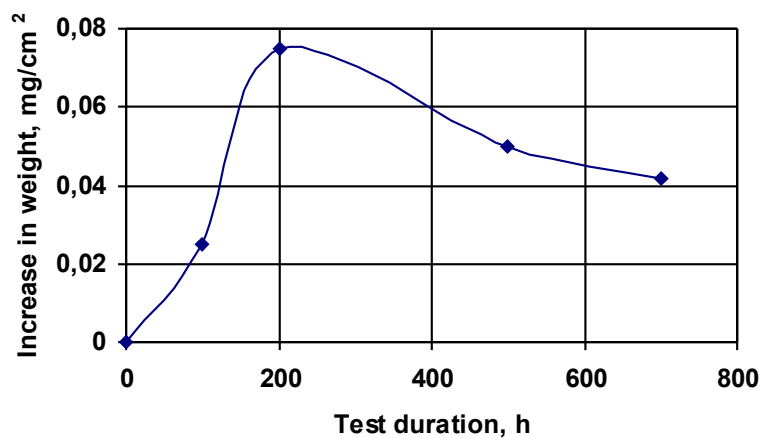


Fig. 4. Time dependence of the increase in weight for the Hastelloy-type alloy samples held in the salt melt at 650°C

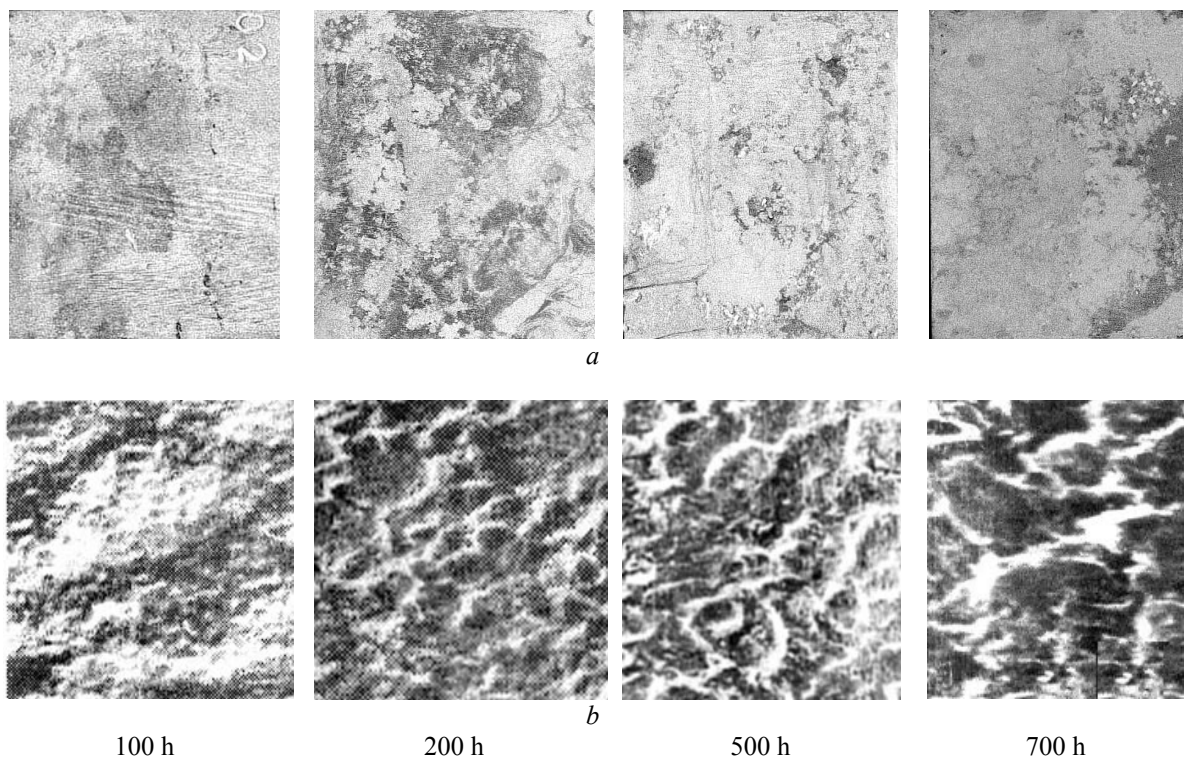


Fig. 5. The appearance of samples and morphological peculiarities of the surface after corrosion tests in the salt melt during 100 to 700 hours: a – appearance of samples (1.3 x magnification); b - morphological peculiarities of sample surfaces (500 x magnification)

Figure 6 shows the microstructure of sample edges after corrosion tests during 100 and 700 hours in the plane perpendicular to rolling. No noticeable signs of intercrystalline corrosion were observed on the samples. The average grain size in the alloy samples is dependent on the time of staying in the salt melt and is found to be 11, 12.6, 14 and 21 μ after 100, 200, 500 and 700 hours of corrosion tests, respectively. Figure 7 shows the mi-

crostructure of samples after corrosion tests in molten salts at 650°C during 100, 200, 500 and 700 hours. The metallographic section surface lies in the plane of rolling.

The mechanical properties of samples after the corrosion tests are presented in Table 1. It is obvious that they remain practically unchanged with increasing time of holding in the molten salts.

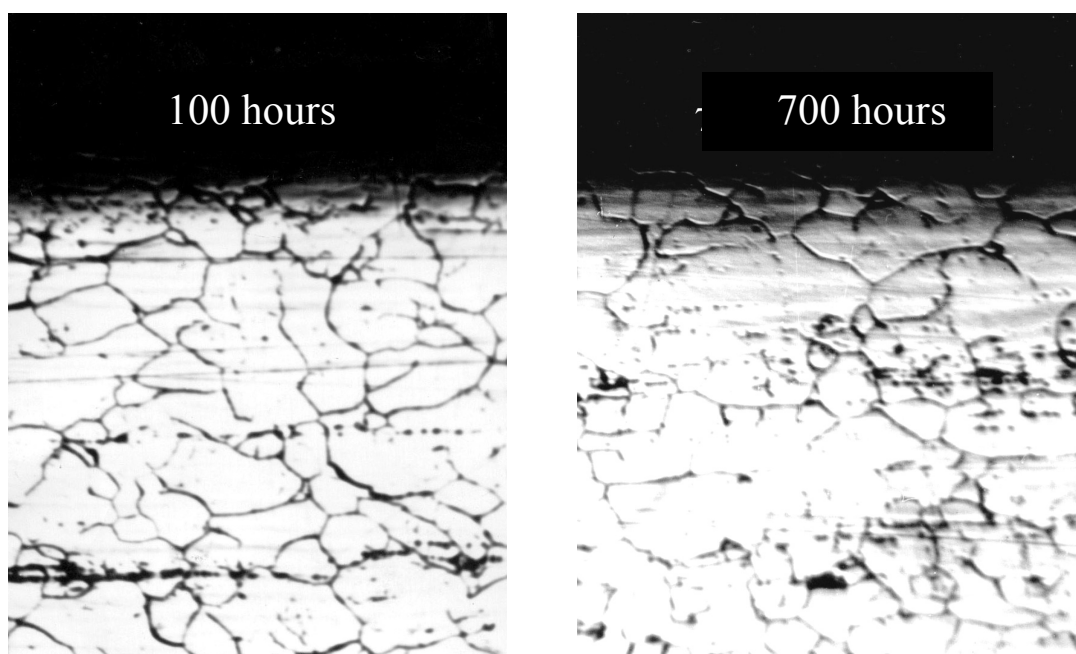


Fig. 6. Microstructure of Hastelloy-type alloy samples after corrosion tests at 650°C during 100 and 700 hours. (380 x magnification)

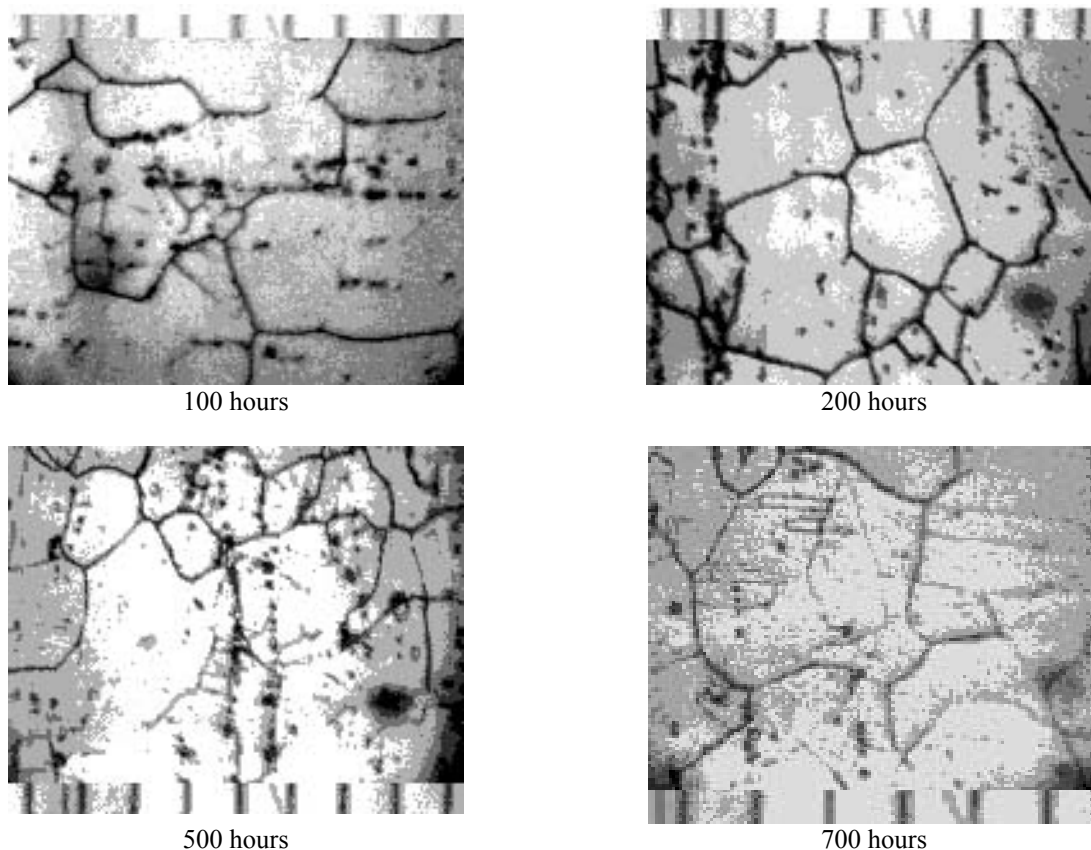


Fig. 7. Microstructure of samples after corrosion tests in molten salts at 650°C during 100, 200, 500 and 700 hours. The scale interval is 10 μm

Table 1

Data from mechanical tests (T = 25, 450 and 650°C) of Hastelloy-type alloy samples subjected to corrosion at 650°C during 100, 200, 500 and 700 hours

Test duration, h	T _{tests} , °C	σ _B , MPa	σ _{0,2} , MPa	δ, %
Initials	25	930	430	60
100		1100	840	41
200		1080	810	45
500		1080	890	43
700		1070	875	43
Initials	450	710	314	62
100		800	400	50
200		800	450	50
500		820	450	50
700		800	460	50
Initials	650	397	288	14
100		502	420	8,0
200		510	435	8,7
500		490	420	10,0
700		510	440	9,0

The secondary-ion mass-spectrometry method was used to investigate the surface composition of the initial alloy sample and the element distribution in the depth of the sample after corrosion tests. A typical spectrum of secondary ions is shown in Fig. 8, where it is seen that the spectrum has all the elements (including isotopes) entering into the alloy composition. To perform quantitative analysis, we have normalized the peak amplitudes of individual elements in conformity with the chemical analysis data. This method enables one to perform the layer-by-layer analysis of the chemical composition of

the alloy, to determine variations in the element concentration versus the thickness of the layer taken off the alloy surface.

Figure 9 shows the spectrum of secondary ions from the sample that underwent corrosion tests in the salt melt at 650°C during 100 hours. The main difference between the two spectra (see Figs. 8 and 9) is that the second spectrum exhibits a large peak of sodium of mass 23, and also peaks of concomitant masses 39 and 40 (NaO, NaOH), which are proportional to the peak value of sodium; and the peaks of masses 90, 91, 92, 94

and 96 associated with zirconium isotopes and of concomitant masses, e.g., 106 (corresponds to $^{90}\text{Zr}^{16}\text{O}$).

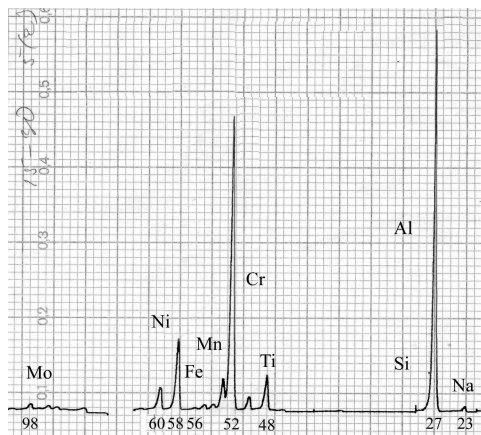


Fig. 8. Typical spectrum of secondary ions from the initial Hastelloy-type alloy sample

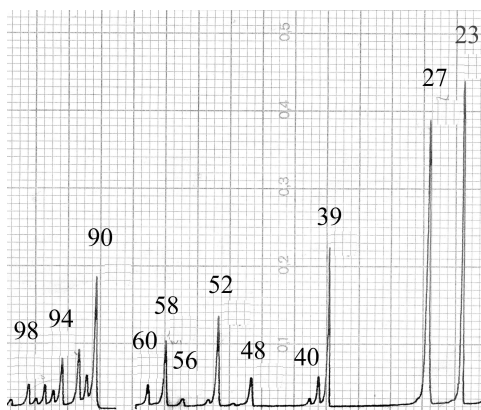


Fig. 9. Typical spectrum of secondary ions from the initial Hastelloy-type alloy sample after staying in the melt of sodium and zirconium fluorides at 650°C during 100 hours

Since they partially overlap with the peaks of molybdenum isotopes, the ^{90}Zr isotope was taken as the basis of measurements (the percentage of this isotope makes 51.46%). Note also the presence of an insignificant peak of fluorine (mass 19) in the second spectrum. The peaks corresponding to the fluorides NaF , ZrF_4 were not observed. The samples that underwent corrosion tests were studied to determine the distribution of the main constituents of the Hastelloy-type alloy: nickel (masses 60 and 58), molybdenum (main isotope of mass 98), chromium (main isotope of mass 52), titanium (main isotope of mass 48), aluminum of mass 27.

It is obvious that after corrosion tests the salt becomes enriched with practically all metals entering into the alloy composition. Figures 10 and 11 show the distributions of titanium and chromium concentrations in the depth of the sample, determined by the secondary-ion emission technique. It can be seen from Fig. 10 that titanium is not practically "washed out" of the sample surface; on the contrary, its concentration increases in the near-surface layer (3 to 10 μm). It is the chromium concentration that is most strongly affected. As it is obvious from Fig. 11, after corrosion tests chromium is washed out from the sample surface to a depth of $\sim 10 \mu\text{m}$.

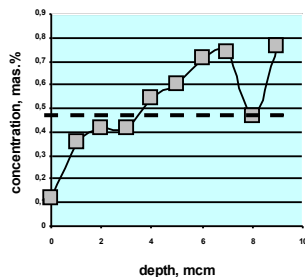


Fig. 10. Titanium concentration variation in the depth of the Hastelloy-type alloy sample after corrosion tests in the molten salts at 650°C during 500 hours. The dashed line shows the initial titanium concentration in the alloy. Separate measurements (shown by squares) are connected by lines for better visualization

Fig. 11. Chromium concentration variation in the depth of the Hastelloy-type alloy sample after corrosion tests in molten salts at 650°C over different periods of time. The dashed line shows the initial chromium concentration in the alloy

The distributions of sodium and zirconium in the depth of the sample held in the salt melt over different periods of time are given in Fig. 12.

It can be seen that as a result of corrosion in the melt of sodium and zirconium fluorides, the penetration of Cr and Zr inside the alloy occurs to a depth of 5 μm .

Chemical analysis of both the initial salt melt and the melt subjected to corrosion tests was performed by the method of laser mass-spectrometry. Table 2 gives the concentrations of titanium, chromium, manganese, iron, nickel and molybdenum in the initial melt of sodium and zirconium fluorides and in the same melt after holding there Hastelloy-type alloy samples at 650°C during 500 hours. These data confirm the results presented in Figs. 10 and 11.

We performed the phase analysis of the Hastelloy-type alloy after corrosion tests in the NaF-ZrF_4 environment at 650°C during 100, 200, 500 and 700 hours. The coolant is based on $7\text{NaF}\cdot 6\text{ZrF}_4$. The results of the analysis are presented in Tables 3 and 4.

According to the data of Table 4, the samples that underwent corrosion tests exhibit the phase $\text{Ni}_3\text{Al}(\text{Ti})$ with a cubic lattice. It is accompanied by the presence of other-stoichiometry compounds NiAl and Ni_2Al_3 . The Ni_3Mo compounds were also observed. The 100-hour exposure gave rise to weak lines at the bottom of the nickel base line (111), which correspond to nickel-aluminum and nickel-molybdenum compounds: NiAl ($2\theta = 44.6$, $d = 2.032 \text{ \AA}$) and Ni_3Mo ($2\theta = 42.8$, $d = 2.113 \text{ \AA}$). Beginning with the

200-hour exposure, traces of NiCr appear. Aside from nickel-containing intermetallides, the sample surfaces also show the traces of the coolant with a crystal structure corresponding to $7\text{NaF}\cdot 6\text{ZrF}_4$.

The second phases manifest themselves most clearly on the sample subjected to the 500-hour exposure. In this case, the sample shows only the $\text{Ni}_3(\text{Al}, \text{Ti})$ phase.

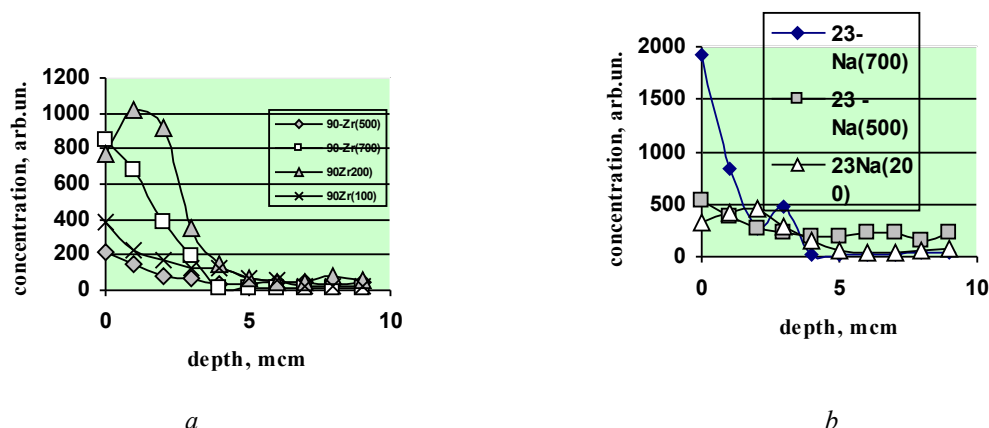


Fig. 12. Element distribution in the depth of the sample after different time periods of staying in the salt melt: a – zirconium; b – sodium

Table 2
Variations in the content of metal impurities in molten salts after corrosion tests at 650°C for 500 hours

Melt	Impurity content, wt. %					
	Ti	Cr	Mn	Fe	Ni	Mo
Initial	<0,0005	0,0039	<0,0005	0,021	0,0031	<0,004
After corrosion	0,007	0,15	0,01	0,21	0,05	0,015

Table 3

Conditional numeration of phases given in Table 4

Phase No	Phase
1	$\text{Ni}_3\text{Al}(\text{Ti})$
2	NiAl
3	Ni_2Al_3
4	Ni_3Mo
5	NiCr
6	$7\text{NaF}\cdot 6\text{ZrF}_4$

Table 4

Phase analysis data for alloy A after corrosion tests at 650°C during 100...700 hours

$d(\text{E})$	Phase No (see Table 3)	Line intensity (%) ¹			
		100 h	200 h	500 h	700 h
3.66	1(3)	1.5	–	–	–
3.175	6	1.5	2.5	1.0	2.0
3.10	6	–	–	3.0	–
2.856	2,3,(6)	1.0	1.5	–	1.0
2.549	1	1.0	1.0	2.5	1.0
2.33...2.36	5	–	1.0	0.5	6.0
2.222	4	0.5	5.0	–	–
$\leq 2.11^2$	4	≥ 3.0	≥ 5.0	≥ 5.0	≥ 4.0
$\geq 2.03^2$	2,3,5	≥ 4.0	≥ 5.0	?	≥ 3.5
1.953	4	0.5	–	0.5	1.0
1.914	6	–	–	0.5	–
1.888	5	–	–	2.5	–
$\leq 1.84^2$	1	–	–	–	≥ 1.0
$\geq 1.82^2$	1	≥ 1.5	≥ 4.0	≥ 2.0	–
1.616	1	1.0	–	1.5	–
Presence of phases No		1–4, 6	1–6	1, 4–6	1–5, (6)

¹The nickel-base line (111) intensity is taken for 100%.

²Lines at the bottom of lines (111) and (200) of the nickel base.

4. CONCLUSIONS

1. Kinetics of Hastelloy-type alloy oxidation in air at temperatures of 650 and 750°C has been investigated. It is found that at oxidation in air the alloy under study is distinguished for its high corrosion resistance superior to the corrosion resistance of steel EI-847. A protective oxide film, up to 1.5 μ in thickness, is formed on the alloy at a temperature of 650°C for 660 hours.
2. The corrosion tests of the Hastelloy-type alloy in the melt of fluorides at 650°C have not revealed any formation of films during a 700-hour corrosion.
3. The process of corrosion of the Hastelloy-type alloy in molten zirconium and sodium fluorides is characterized by weak interaction of melt components with the alloy, by penetration of Zr and Na atoms into the alloy to a depth of 3 ... 5 μ m over a period of 700 hours, by the absence of oxide films on the surface. A decrease of chromium concentration in the near-surface layer of the alloy to a depth of ~ 10 μ m occurs.
4. The present corrosion tests have caused no essential changes in the mechanical properties of the alloy.
5. The samples that underwent corrosion tests have exhibited the Ni₃Al(Ti) phase with a cubic lattice. Along with this phase, other-stoichiometry compounds NiAl and Ni₂Al₃ were present. The Ni₃Mo compounds and the traces of the NiCr phase were also observed.

This work was partially supported by the STCU, Project #294.

- 1.V.L. Blinkin, V.M. Novikov. *Molten-salt nuclear reactors* (in Russian). Moscow: "Atomizdat publ." 1978, 112 p.
- 2.V.M. Novikov, V.V. Ignatyev, V.I. Fedulov, V.N. Cherednikov. *Molten-salt NEF: prospects and problems* (in Russian). Moscow: "Ehnergoizdat", 1990, 192 p.
- 3.U.R. Grims. *Problems of materials choice for molten-salt reactors* (Russian translation). Moscow: "Atomizdat publ." 1966, p. 69–98.
- 4.V.M. Azhazha, Yu.P. Bobrov, V.D. Virich, et al. Refinement of nickel by electron-beam melting (in Russian) // *Kharkov University Bulletin. Ser. phys.: "Nuclei, particles, fields"*. 2003, N601, is. 2(22), p. 118–122.
- 5.V.M. Azhazha, Yu.P. Bobrov, P.N. V'yugov, et al., Development of the alloy for the fuel loop of molten-salt reactors (in Ukrainian) // *Kharkov University Bulletin. Ser. phys.: "Nuclei, particles, fields"*. 2004, is. 1(23), p. 87–94.
- 6.V. Azhazha, A. Bakai, S. Lavrinenko, Yu. Bobrov et al., Alloys for molten-salt reactors (in Ukrainian) // *Proceedings of the XVI International conference on physics of radiation phenomena and radiation materials science. 6 – 11 September, 2004, Alushta, Crimea, NSC KIPT*, p. 271–272.
- 7.V. Azhazha, A. Bakai, Yu. Bobrov, S. Lavrinenko, I. Petel'guzov, V. Savchenko. Investigation of corrosion resistance and mechanical properties of high-temperature heat-resistant nickel alloy (in Russian) // *Fracture mechanics of materials and structural strength. Ed. by V.V. Panasyuk. L'viv, G.V. Karpenko Institute for Physics and Mechanics, National Academy of Sciences in Ukraine*, 2004, p. 659–664.

REFERENCES

КОРРОЗИОННАЯ СТОЙКОСТЬ ЖАРОПРОЧНОГО НИКЕЛЕВОГО СПЛАВА В РАСПЛАВАХ ФТОРИДНЫХ СОЛЕЙ

В.М. Ажажа, А.С. Бакай, Ю.П. Бобров, В.Д. Вирич, Т.Г. Емлянинова, В.Л. Капустин, К.В. Ковтун, С.Д. Лавриненко, Д.Г. Малыхин, И.А. Петельгузов, Н.Н. Пилипенко, В.И. Савченко, Н.А. Семенов, А.Д. Солопихин, Б.М. Широков

Исследовались коррозионные и механические свойства образцов высоконикелевых сплавов, которые были изготовлены в ННЦ ХФТИ на основе высокочистых металлических компонентов. В результате коррозионных испытаний сплава типа Хастеллой в расплаве фторидов при температуре 650°C не обнаружено образования каких-либо плёнок в процессе коррозии в течение 700 ч. Процесс коррозии этого сплава в расплавах фторидов характеризуется слабым взаимодействием компонентов смеси со сплавом, проникновением атомов Zr и Na в сплав на глубину до 3...5 мкм за время 700 ч, отсутствием оксидных плёнок на поверхности. Происходит уменьшение концентрации хрома в приповерхностном слое сплава на глубину до 10 мкм. Коррозионные испытания не приводят к значительному изменению механических свойств сплава.

КОРОЗИЙНА СТІЙКІСТЬ ЖАРОМІЦНОГО НІКЕЛЕВОГО СПЛАВУ В РОЗПЛАВАХ ФТОРИДНИХ СОЛЕЙ

В.М. Ажажа, О.С. Бакай, Ю.П. Бобров, В.Д. Вірич, Т.Г. Емлянінова, В.Л. Капустин, К.В.Ковтун, С.Д. Лавриненко, Д.Г. Малихін, І.А. Петельгузов, М.М. Пилипенко, В.І. Савченко, М.О. Семенов, А.Д. Солопихін, Б.М. Широков

Досліджувалися корозійні і механічні властивості зразків високонікелевих сплавів, які були виготовлені в ННЦ ХФТИ на основі високочистих металевих компонентів. В результаті корозійних випробувань сплаву типу Хастеллой в розплаві фторидів при температурі 650°C не знайдено утворення яких-небудь плівок в процесі корозії протягом 700 г. Процес корозії цього сплаву в розплавів фторидів характеризується слабкою взаємодією компонентів суміші із сплавом, проникненням атомів Zr і Na в сплав на глибину до 3...5 мкм за час 700 г, відсутністю оксидних плівок на поверхні. Від-

бувається зменшення концентрації хрому в при поверхневому шарі сплаву на глибину до 10 мкм. Корозійні випробування не призводять до значної зміни механічних властивостей сплаву.